

Elevation-dependent sensible heat flux trend over the Tibetan Plateau and its possible causes

Lihua Zhu, Gang Huang, Guangzhou Fan, Xia Qü, Zhibiao Wang & Wei Hua

Climate Dynamics

Observational, Theoretical and Computational Research on the Climate System

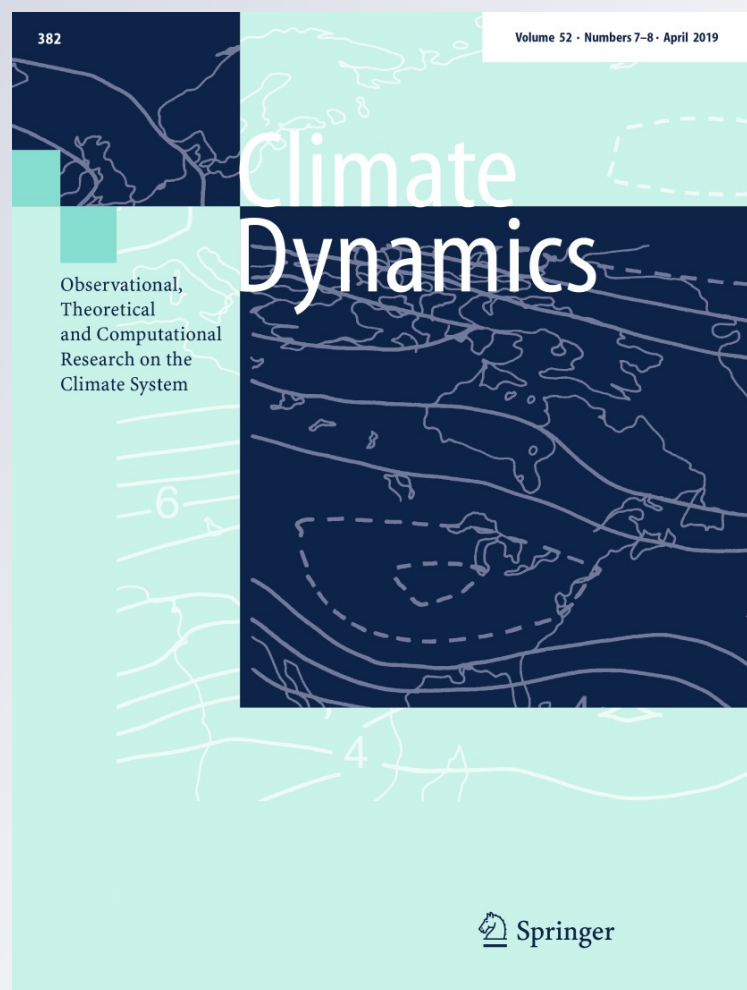
ISSN 0930-7575

Volume 52

Combined 7-8

Clim Dyn (2019) 52:3997-4009

DOI 10.1007/s00382-018-4360-7



Your article is protected by copyright and all rights are held exclusively by Springer-Verlag GmbH Germany, part of Springer Nature. This e-offprint is for personal use only and shall not be self-archived in electronic repositories. If you wish to self-archive your article, please use the accepted manuscript version for posting on your own website. You may further deposit the accepted manuscript version in any repository, provided it is only made publicly available 12 months after official publication or later and provided acknowledgement is given to the original source of publication and a link is inserted to the published article on Springer's website. The link must be accompanied by the following text: "The final publication is available at link.springer.com".



Elevation-dependent sensible heat flux trend over the Tibetan Plateau and its possible causes

Lihua Zhu^{1,2,3} · Gang Huang^{2,3,4,5} · Guangzhou Fan^{1,6} · Xia Qū⁷ · Zhibiao Wang^{3,7} · Wei Hua¹

Received: 10 February 2018 / Accepted: 15 July 2018 / Published online: 28 July 2018
© Springer-Verlag GmbH Germany, part of Springer Nature 2018

Abstract

The present study documents the elevation-dependent sensible heat (SH) flux trend over the Tibetan Plateau (TP). The SH displays a decreasing trend over the TP above 2000 m with the magnitude of trend increasing with the elevation, but an increasing trend at low elevation stations. The above feature is more obvious in spring and summer. Surface wind speed is consistently the major contributor to the variation in SH trend from lower to higher altitude areas. Meanwhile, the role of the difference of ground-air temperature ($T_s - T_a$) in SH trend is enhanced above 2500 m regions. The SH variation associated with the change in $T_s - T_a$ may be influenced primarily by the diminution in sunshine duration and snow depth at higher-altitude regions, and the latter is particularly important. The portion of the SH variation related to the change in surface wind speed is mainly attributed to the dynamic process related to the Pacific Decadal Oscillation (PDO). The warming in the northwestern Pacific in relation to the switch of the PDO from a warm phase to a cold phase in the recent decades causes divergence anomalies in the upper troposphere, which induces propagation of a wave pattern extending eastward until reaching the southwest TP. That leads to an enhancement in divergence of the upper troposphere and subsequently a boost in surface convergence and rising motion over southwest TP. Consequently, due to the easterly anomaly to the east of the convergence, surface wind speed is reduced over the central and eastern TP, especially in the higher altitude areas.

Keywords Altitude dependence · Surface sensible heat trend · Tibetan Plateau · The difference of ground-air temperature · Surface wind speed

1 Introduction

It is well known that solar radiation is the source of surface energy, and the solar irradiance heavily relies on the status of underlying surface—terrain height, for instance. The higher the elevation, the more the solar irradiance reaching the Earth's surface due to less absorption and reflection

of solar radiation by the atmosphere. In turn, the increased difference of ground-air temperature brings about the heat transmission from surface land to air in the form of sensible heat (SH). Consequently, the SH over the plateau tends to be particularly striking.

The Tibetan Plateau (TP) is world-renowned for its vast acreage, high altitude, and extremely complex terrain. It

✉ Gang Huang
hg@mail.iap.ac.cn

¹ School of Atmospheric Sciences/ Plateau Atmosphere and Environment Key Laboratory of Sichuan Province/Joint Laboratory of Climate and Environment Change, Chengdu University of Information Technology, Chengdu 610225, China

² State Key Laboratory of Numerical Modeling for Atmospheric Sciences and Geophysical Fluid Dynamics, Institute of Atmospheric Physics, Chinese Academy of Sciences, Beijing 100029, China

³ University of Chinese Academy of Sciences, Beijing 100049, China

⁴ Laboratory for Regional Oceanography and Numerical Modeling, Qingdao National Laboratory for Marine Science and Technology, Qingdao 266237, China

⁵ Joint Center for Global Change Studies, Beijing 100875, China

⁶ Collaborative Innovation Center on Forecast and Evaluation of Meteorological Disasters, Nanjing University of Information Science and Technology, Nanjing 210044, China

⁷ Center for Monsoon System Research, Institute of Atmospheric Physics, Chinese Academy of Sciences, Beijing 100029, China

exerts a great influence on regional and even global climate via its thermal and dynamic forcing mechanism (Yeh et al. 1957; Yeh and Gao 1979; Yanai et al. 1992; Ye and Wu 1998; Chakraborty et al. 2002, 2006; Duan and Wu 2005; Boos and Kuang 2010; Duan et al. 2012; Wu et al. 2012a, 2014; Yao et al. 2012). As a huge heat source towered in the free atmosphere, the TP transfers heat from surface land to the air in the form of sensible heat and latent heat transfer, and effective radiation of the ground, among which SH makes the maximum contribution annually, especially in spring and summer (Yeh et al. 1957; Yeh and Gao 1979; Duan and Wu 2008; Yang et al. 2011a; Wu et al. 2014). During spring and summer, the water vapor and air mass in the low level atmosphere around the plateau are suctioned to the TP, converging and ascending there. All of these are driven by the heating, which is vividly described as Sensible Heating Atmosphere Pumping (SHAP; Wu et al. 1997, 2007, 2014). The SH is one of the crucial important causes for triggering the convective precipitation and the latent heat release over the TP and its downstream regions (Wan and Wu 2007; Wu et al. 2007, 2012b, 2014, 2016; Wan et al. 2009; Duan et al. 2011, 2013; Liu et al. 2012; Wang et al. 2014). What's more, the TP, reputed as the Asian water tower, is the cradle of many prominent Asian rivers (Immerzeel et al. 2010; Yao et al. 2012). The precipitation on the plateau and its lower reaches has a remarkable impact on the river runoff, the lake water level, and even more on the drought and waterlogging in its downstream regions. The SH also has a notable effect on the onset and intensity of the Asian summer monsoon (Wu et al. 2012a, c, 2014, 2016; Liu et al. 2013; Duan et al. 2013). In addition, the SH over the TP can also exert an influence on the evolution of global atmospheric circulation and the abnormal of climate by means of Rossby wave dispersion (Wu et al. 2012a, 2014, 2016; Wang et al. 2014).

Accordingly, the variation in SH over the TP has important implications for the redistribution of energy and the exchange of momentum, for the change of heat and moisture transmission between the land and atmosphere, for the hydrologic cycle over the TP and its downstream regions, and also for the evolution of the atmospheric circulation and the anomaly of the climate for regional and even global. What's more, all of these plateau's pivotal roles are closely correlated with its height. In other words, the distinct SH over the TP, compared with that on flat land, should give the credit to high elevation to a large extent. The mechanism of elevated heating has been demonstrated in studies (Yeh and Gao 1979; Molnar and Emanuel 1999; Wu et al. 2014; Hu and Boos 2017a, b). However, the analysis on the spatial variation of the SH over the TP is prone to be confined to the horizontal dimension (e.g., Duan and Wu 2008; Duan et al. 2011). It was mentioned in the articles that perhaps the trend in SH was related to elevation in spring (Duan et al. 2011), but the trends in all variables associated with SH may not

be directly related to elevation (Wang et al. 2012). However there were no details about the change of SH with the elevation. It is still unclear whether the trend of SH over the TP has an altitude dependence or not, and what is the major contributor to it. Hence, this article will give an explicit demonstration about it, and that will help to better assess energy fluxes and moisture availability at the land surface.

The overall structure is as follows. Section 2 described briefly the data and methodology applied in this study. The elevation-dependency of the trend in SH over the TP is introduced in Sect. 3 and the possible causes are discussed in Sect. 4, followed by summary and discussions in Sect. 5.

2 Data and methodology

2.1 Data

The data used in this study comprise: the regular surface meteorological observations for the TP area offered by the China Meteorological Administration (CMA), in which the variables of four times daily consist of ground surface temperature (T_s), surface air temperature (T_a), wind speed at 10 m above the surface (V_0), and daily snow depth and sunshine duration; monthly mean U wind component, V wind component, vertical velocity, air temperature, and geopotential of the European Centre for Medium-Range Weather Forecast Interim Reanalysis (ERA-Interim; Dee et al. 2011) at a horizontal resolution of $1^\circ \times 1^\circ$; monthly SST data during the same period from the Met Office Hadley Centre Sea Surface Temperature (HadISST) dataset (Rayner et al. 2003), provided at a resolution of $1^\circ \times 1^\circ$ (<http://hadobs.metoffice.com/hadisst/data/download.html>); daily normalized difference vegetation index (NDVI) from NOAA Climate Data Record Program (Pedelty et al. 2007), with a resolution of $0.05^\circ \times 0.05^\circ$ (<https://www.ncdc.noaa.gov/cdr/terrestrial/normalized-difference-vegetation-index>); the PDO index is obtained from <http://research.jisao.washington.edu/pdo>.

The data periods above are all from January 1980 to December 2015, except for NDVI covering 1981–2014.

The locations and elevations of the stations involved in the present analysis are shown in Fig. 1, most of which are located in Qinghai, Xizang, Gansu and the western Sichuan in China. This dataset covers the domain of TP with 140 stations, and in general, the missing values of variables account for less than 0.5% of the total records. The method of processing missing values in data is the same as applied in Duan and Wu (2008). To ascertain the elevation dependent variation of SH over TP, the 140 stations were divided into 8 altitudinal ranges with a 500 m interval. The number of stations and the average elevation in each range are listed in Table 1. Among these stations, 82 (58.6%) are above 2000 m, 48 (34.3%) above 3000 m, and

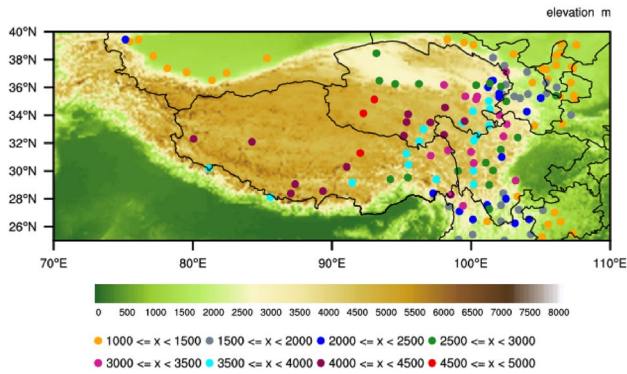


Fig. 1 The locations and elevations for stations in 500-m-wide altitudinal bands starting at 1000 m

16 (11.4%) above 4000 m, which is sufficient for identifying and quantifying the elevation-dependency of SH notwithstanding the sparse high-elevation observations.

2.2 Methods

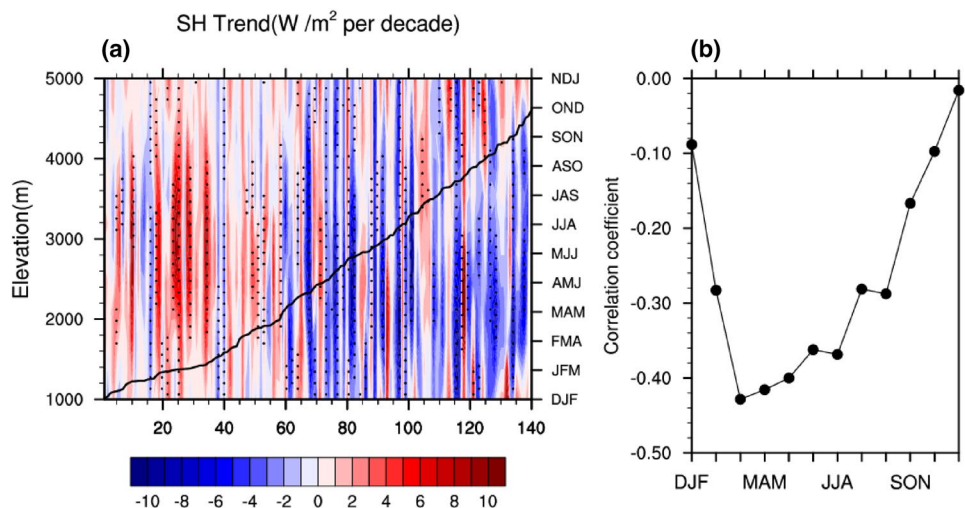
The SH is calculated by the bulk aerodynamic method, which is widely applied in many studies related to TP (e.g., Yeh and Gao 1979; Chen et al. 1985; Li et al. 2001; Duan and Wu 2008; Duan et al. 2011, 2013; Cui et al. 2015; Zhu et al. 2017):

$$SH = C_p \rho_a C_{DH} V_0 (T_s - T_a)$$

Table 1 Number of stations and average elevation for eight altitudinal ranges

Altitudinal range (km)	1–1.5	1.5–2	2–2.5	2.5–3	3–3.5	3.5–4	4–4.5	4.5–5
Number of stations	36	22	16	18	15	17	13	3
Mean elevation (m)	1282	1774	2314	2785	3251	3735	4199	4551

Fig. 2 a Elevation-dependent variation of trend for SH of 140 stations during 1980–2015. The black bold curve denotes elevation. Values exceeding the 95% significance level are presented in dots. **b** Correlation coefficients between SH trends and elevations of 140 stations



Descriptions of the physical quantities in the above formula are available in the referenced literature. In this study, $C_p = 1005 \text{ J kg}^{-1} \text{ K}^{-1}$ is the specific heat of dry air at constant pressure. The changes in the air density (ρ_a) should be subtle during the study period from 1980 to 2015 (Zhu et al. 2017), as well as the drag coefficient for heat (C_{DH}), and their influence on the variation of SH is negligible though they vary from location to location. Thus, we assume $C_{DH} = 4 \times 10^{-3}$ for the east of 85°E and $C_{DH} = 4.75 \times 10^{-3}$ for the west of 85°E (Li and Yanai 1996; Duan and Wu 2008; Duan et al. 2011, 2013; Zhu et al. 2017), and $\rho_a = 0.8 \text{ kg m}^{-3}$ (Yeh and Gao 1979; Duan and Wu 2008; Duan et al. 2011, 2013). Consequently, in the procedure above, out of the three constants, the surface wind speed (V_0) and the difference in ground-air temperature ($T_s - T_a$), as the focus of this article, are the key factors influencing the evolution of SH.

3 Elevation-dependent variation of SH trend

The trend of SH from 140 stations over TP shows that most of the stations have experienced statistically significant decreasing trend during 1980–2015 except for some stations below 2000 m elevation (Fig. 2a). The higher the altitude, the larger the negative trend. This elevation dependence feature is most obvious in spring. It is partially consistent with the conclusion mentioned in previous literature (Duan et al. 2011). The correlation coefficients between SH trends and elevations of 140 stations in spring and summer are

−0.42 (at the 99% confidence level) and −0.37(at the 99% confidence level), respectively, which are larger than those in autumn (−0.17) and winter (−0.09) (Fig. 2b). The elevation-dependence of the SH trend in spring principally results from more prominent decreasing trend in SH at higher altitude, while that in summer is chiefly caused by larger trend at lower altitude.

To investigate the reason for the elevation dependency of SH trend, the trends of SH and relative variables for stations in 500-m-wide altitudinal bands during different seasons are given in Fig. 3. Refer to Table 1 for the details

about the ranges. Considering that there are only three stations above 4500 m and there is a narrow margin between their mean elevation and 4500 m, here the stations at the ranges of 4000–4500 and 4500–5000 m are merged together in Fig. 3. The SH weakens more strikingly as altitude goes up, especially in spring and summer (Fig. 3a), confirming the conclusions of the figure above. Compared with $T_s - T_a$, the altitude dependence of V_0 trend over the TP (Fig. 3b) is more approximate to the variation in SH. The decreasing trend in V_0 is amplified with elevation in the four seasons, most notable in springtime. This conclusion is in accord with

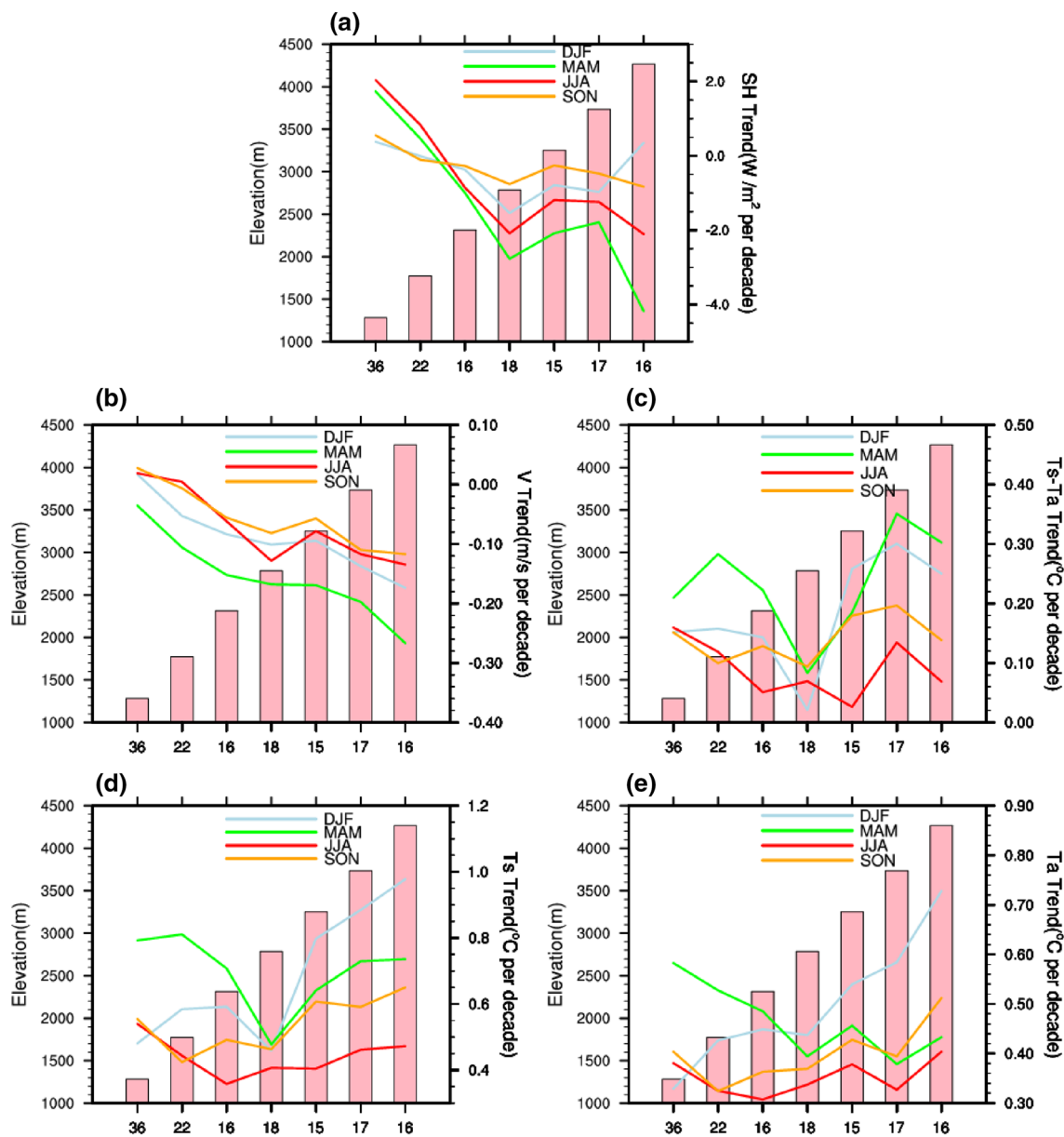


Fig. 3 Elevation-dependent variation for trends of SH and relative variables over TP during 1980–2015 for DJF, MAM, JJA, and SON. Bars represent elevations and trend magnitude is plotted on the y axis

of right side according to the 7 elevation ranks of 140 stations. Number of stations in each elevation group is plotted on the x axis of bottom

the result of existing literature (Guo et al. 2017). In addition, the change of the trend in $T_s - T_a$ with altitude is related to the elevation-dependent variation in trend of T_s considerably. The positive trend of $T_s - T_a$ increases as the altitude ascends above 2500 m (Fig. 3c) owing to the elevation dependence of warming in T_s there (Fig. 3d). But there was no strong elevational effect for T_a in other seasons except in winter and autumn (Fig. 3e), which is consistent with the results in previous literature (Yan and Liu 2014; Pepin et al. 2015). Various mechanisms and processes have been linked to the elevation-dependent warming. The most common explanation is associated with the snow-albedo feedback mechanism (Giorgi et al. 1997; Pepin and Lundquist 2008; Ceppi et al. 2010; Kothawale et al. 2010), moreover, water vapour and radiative fluxes (Philipona et al. 2005; Rangwala et al. 2009, 2010; Rangwala 2013), the cloud-radiation effects (Liu et al. 2009) and so on, are also responsible for it.

Does the variation in Fig. 3 indicate that wind speed is the main reason affecting altitude dependence of SH trend? Partial correlation (Zar 1999; Saiji and; Yamagata

2003; Hu and Duan 2015) between SH trend and the relevant variable trend ($T_s - T_a$ or V_0) of every successive 41 stations is calculated sliding along the low-to-high elevation order (Fig. 4) to quantitatively analyze the relative importance of $T_s - T_a$ and V_0 to elevation-dependence of SH trend. On average, the effect of $T_s - T_a$ and V_0 on elevation-dependence of SH trend is similar in winter and autumn (Fig. 4a, d). Nevertheless, V_0 is the major contributor to the variation in SH trend in spring and summer (Fig. 4b, c). Meanwhile, it is noteworthy that the role of $T_s - T_a$ in altitude-dependence of SH trend is enhanced in the regions above 2500 m. Moreover, the partial correlation between SH trend and V_0 trend sliding along the low-to-high elevation order shows small change with altitude in spring and summer. Thus it can be seen that the influence of V_0 trend on SH tendency may not be directly related to elevation despite notable. In other words, V_0 is a stable contributor to the variation in SH trend from lower to higher altitude areas. While the effect of $T_s - T_a$ on SH is more striking at higher altitude starting at 2500 m in springtime.

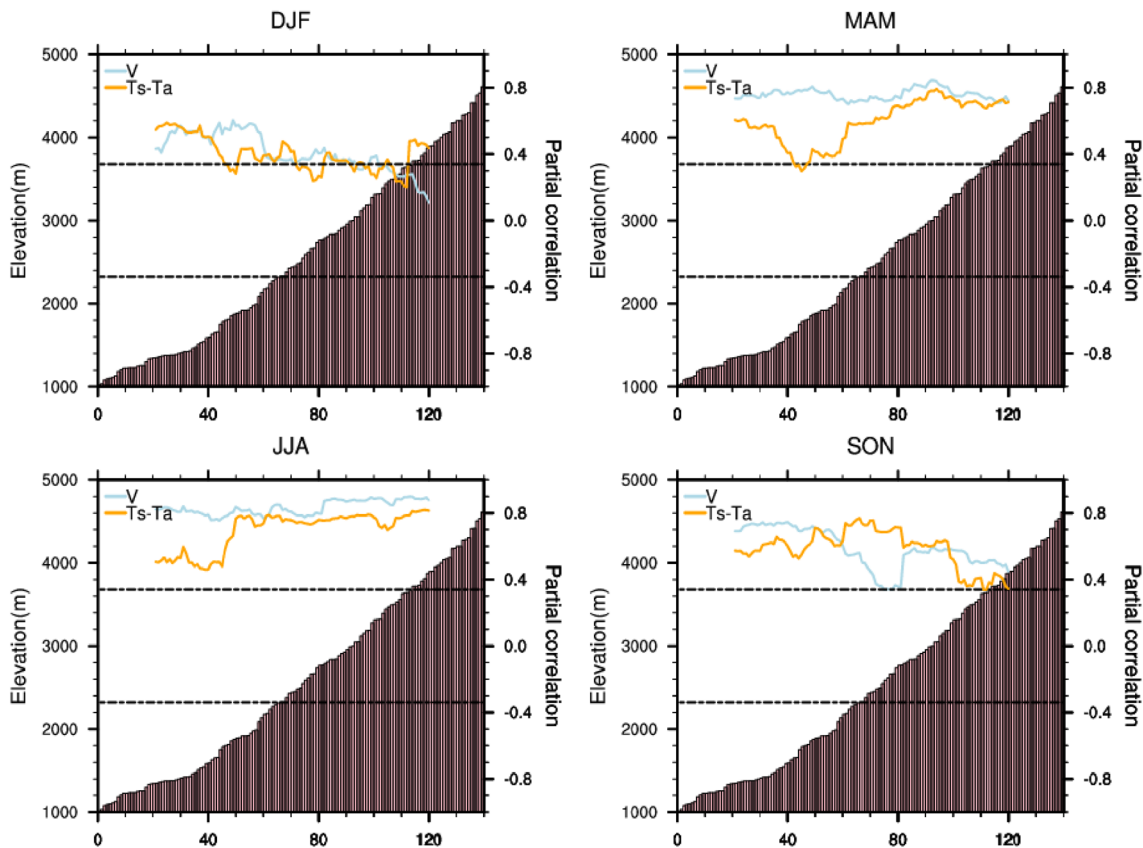


Fig. 4 Partial correlation between SH trend and various factor trend ($T_s - T_a$ and V_0) of every successive 41 stations sliding along the low-to-high elevation order. Bars represent elevation and partial correla-

tion magnitude is plotted on the y axis of right side. Black dashed line indicates the 95% significance level

4 Cause for elevation dependency of SH trend

What factors influence the elevation-dependent variation of SH over the TP by affecting V_0 or $T_s - T_a$? Relatively high value of SH over the TP appears in spring, and so does the notable altitude dependence of SH trend. Consequently, here we take spring as an example to demonstrate. Three potential factors are analyzed in this study: sunshine duration that is a factor affecting on the amount of solar radiation reaching the earth's surface (Stanhill and Cohen 2005; Sanchez-Lorenzo et al. 2008; Matuszko 2014; Founda et al. 2014; Manara et al. 2015), snow depth that is a factor influencing surface albedo (Pedersen and Winther 2005; Flanner et al. 2011; Fletcher et al. 2012), and NDVI that is a factor impacting on surface roughness (Bastiaanssen et al. 1998; Hong et al. 2009; Zheng et al. 2014).

The trend in MAM for sunshine duration, snow depth, and NDVI are exhibited in Fig. 5, as well as the correlation coefficients between SH trend and the three variable trend

(sunshine duration, snow depth, and NDVI) of every successive 41 stations sliding along the low-to-high elevation order. To facilitate analysis, NDVI used in Fig. 5 has been interpolated from high resolution grid to sites. The trend of sunshine duration is highly and positively correlated with that of SH, with a correlation coefficient of 0.45, exceeding the 99% confidence level (Fig. 5a). In addition, the higher the altitude, the larger the positive correlation is, especially above 2500 m (Fig. 5d). The sunshine duration in the region above 2500 m mainly presents a decreasing tendency (Fig. 5a). It lessens the amount of solar short-wave radiation reaching earth's surface. Because of the smaller specific heat capacity on the ground compared with air in general, the reduced downward solar short-wave radiation eventually results in a distinct reduction in T_s than T_a , and even $T_s - T_a$, and what's more, diminution in SH.

A significant negative correlation exists between the trend of snow depth and SH, with correlation coefficient of -0.38 (99% confidence level). And it is more striking in snow-dominated higher elevation regions (Fig. 5d). There the snow depth of the surface has declined under the background

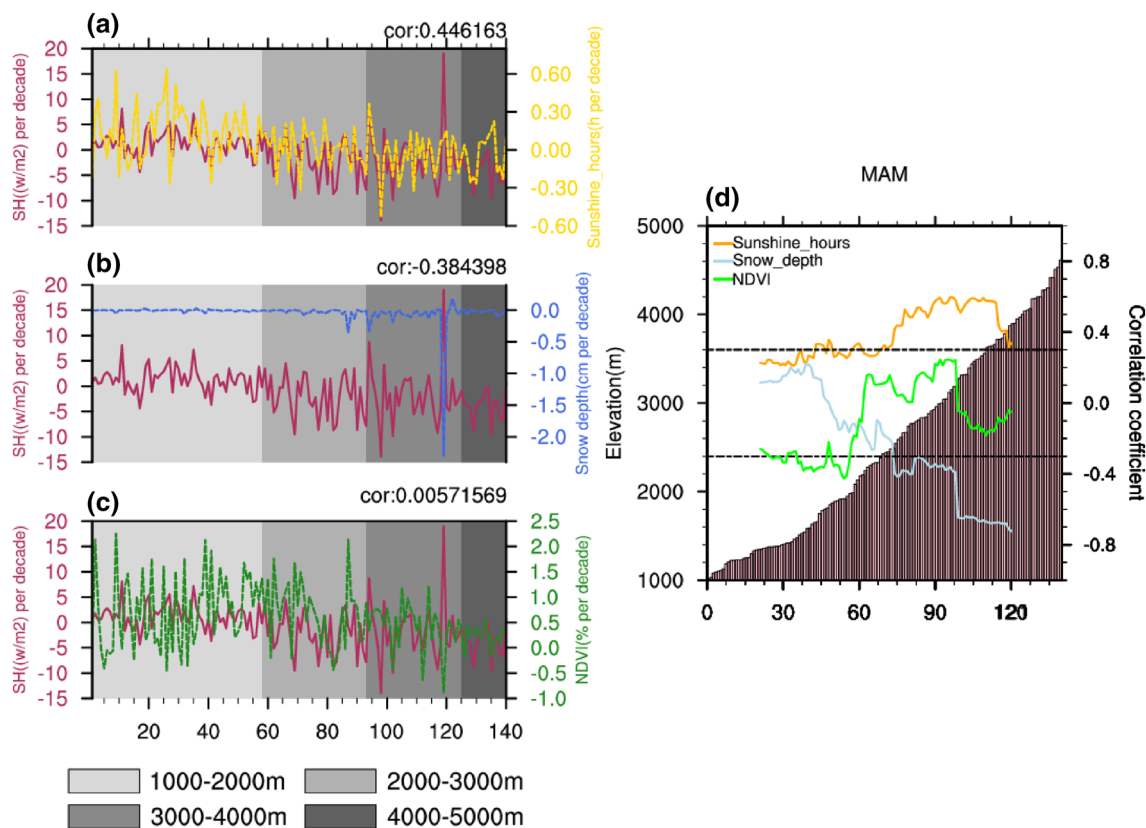


Fig. 5 Elevation-dependent variation of trend in MAM for SH, a sunshine duration, snow depth and c NDVI of 140 stations during 1980–2015. Altitudinal range is expressed in gray. **d** Correlation coefficients between the SH trend and various factor trend (sunshine dura-

tion, snow depth, and NDVI) of every successive 41 stations according to the low-to-high elevation order. Bars represent elevation and correlation coefficient magnitude is plotted on the y axis of right side. Black dashed line indicates the 95% significance level

of global warming (Fig. 5b), which leads to the changes in surface absorption of solar radiation and the enhancement of warming over higher altitude. The increment in T_s is greater than that in T_a , which leads to the augmentation of $T_s - T_a$ and even SH. The trend of $T_s - T_a$ shown in Fig. 3 increases with the altitude in higher-elevation regions (above 2500 m). In other words, the variation in SH contributed by the change of $T_s - T_a$ may be influenced primarily by the diminution in snow depth, especially at higher-altitude regions.

The correlation between the trend of NDVI and SH is small whether in lower or higher altitude areas (Fig. 5c). Accordingly, the portion of variation in SH dedicated by the change of V_0 is less related to the surface roughness. Then what has led to the weakened V_0 associated with SH in the higher altitude regions over the TP?

The U wind component and V wind component are calculated using wind direction and wind velocity of surface meteorological observations. And their variation in trends are demonstrated in Fig. 6a, b. The U wind component makes a substantial contribution to the decreasing wind speed in the higher altitude areas (above 2000 m) over the TP (Fig. 6a). Additionally, the dwindling V wind component in the southeastern Tibetan Plateau has also contributed to the weakened wind speed in some extent (Fig. 6b). While the incremental wind speed sporadically distributed in the lower elevation areas on the eastern side of the TP is benefit from the combined action of U and V wind component.

To demonstrate the cause of attenuated wind over the TP, the ERA-Interim dataset is used in this part. On the average,

there are northwesterly and southwesterly winds converging on the TP (Fig. 6c). Compared with the climate mean state, the spatial pattern of linear trend for wind indicates that wind speed, especially U wind component, decreases in the higher altitude areas. And simultaneously there are accelerated easterly or southeasterly winds in the lower elevation regions on the eastern side of the TP (Fig. 6d). It is thus evident that the ERA-Interim fits well with observations.

The anomalous atmospheric circulation often tends to have a direct influence on the change of wind velocity. There is an abnormal convergence over the western plateau, as shown in the blue rectangle of Fig. 6d, correspondingly it exhibits easterly anomaly to the east of it. And it reduces the surface wind speed over the central and eastern TP, especially in the higher altitude areas. Consequently, the abnormal convergence mentioned above may be the immediate cause of the decreasing surface wind speed on the higher altitude areas. Then quasi-geostrophic ω equation (Eq. 1) is utilized in this section to diagnose the principal cause of the upward motion associated with surface convergence mentioned above. The terms on the right side of the Eq. (1) express respectively the variation of vorticity advection with height (B), Laplace for temperature advection (C), and Laplace for diabatic heating (D). And the regression fields of the wind (vectors) at 10 m with respect to them are shown in Fig. 7. Compared to regression field based on temperature advection (Fig. 7c) and diabatic heating (Fig. 7d), the vector pattern regressed on the absolute vorticity advection (Fig. 7a) displays a stronger

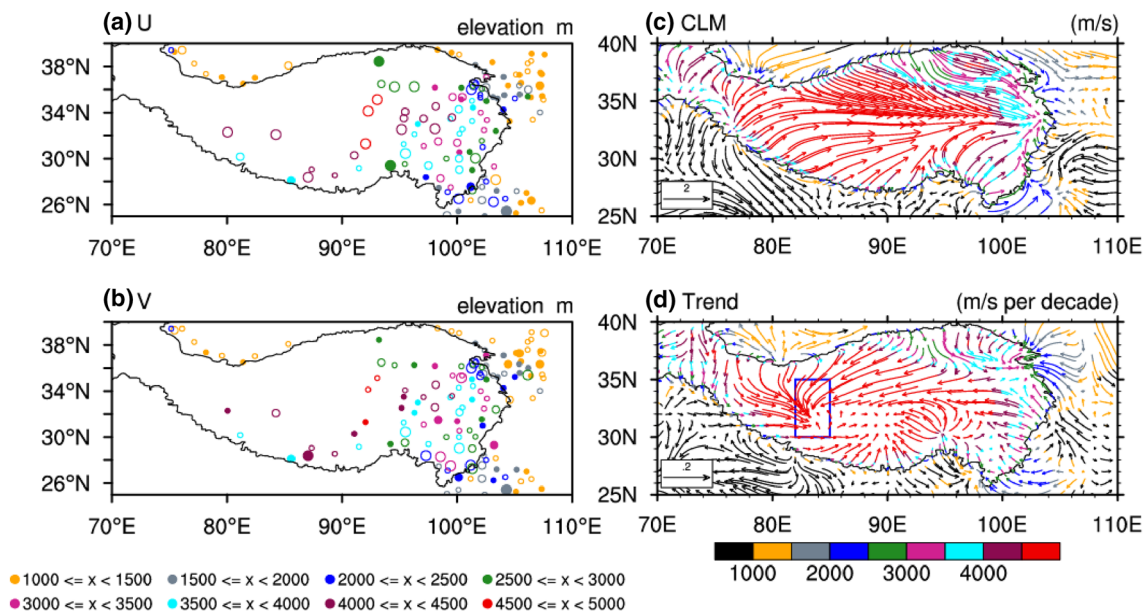


Fig. 6 Spatial distribution for the product of the linear trend and the symbol of climatological mean for **a** U wind component and **b** V wind component. The hollow circle represents negative value, and the solid circle represents positive value. The bigger the circle, the larger

the absolute value is. **c** Climatological mean and **d** linear trend of the wind (vectors) at 10 m in MAM during 1980–2015 for the ERA-Interim. Altitudinal ranges are expressed in colors

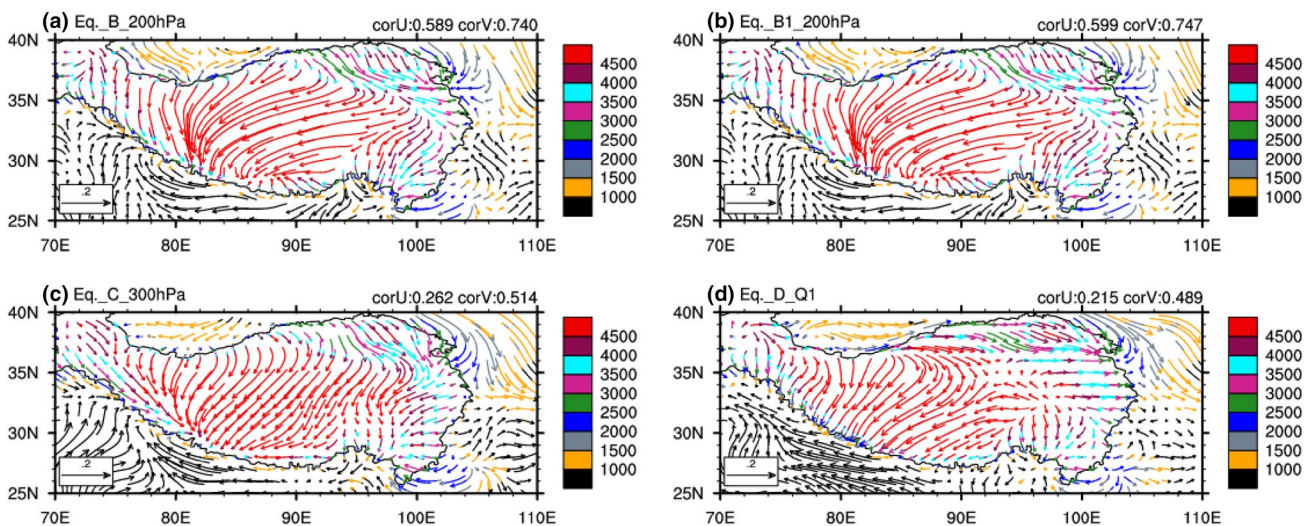


Fig. 7 Regression pattern of the wind(vectors) at 10 m regressed on **a** the variation of absolute vorticity advection with height, **b** the variation of relative vorticity advection with height, **c** Laplace for temperature advection, and **d** diabatic heating integrated vertically from

500to100 hPa. The correlation coefficient between the regression pattern and the linear trend field in Fig. 6d are shown in the upper right corner of each graph

resemblance with the field of linear trend for wind at 10 m (Fig. 6d). It makes clear that compared with the other two items, the increased vorticity advection with height is a more important contributor to the anomalous surface wind velocity reinforcing the convergence upward movement over the southwest TP (Fig. 7a). Among which, relative vorticity advection plays a pivotal role, and the correlation coefficient between the regression pattern (Fig. 7b) and the linear trend field (Fig. 6d) is 0.599 for U wind component and 0.747 for V wind component, both exceeding the 99% confidence level. This indicates that the abnormal wind speed associated with SH over the TP mainly is due to dynamic process. With regard to the interdecadal change of the wind speed closely related to the variation of SH over the TP, what may be responsible for it?

$$\underbrace{\left(\sigma \nabla^2 + f^2 \frac{\partial^2}{\partial p^2}\right)}_A \omega = f \underbrace{\frac{\partial}{\partial p} \left[\vec{V}_g \cdot \nabla (\zeta_g + f) \right]}_B$$

$$+ \underbrace{\frac{R}{p} \nabla^2 \left[\vec{V}_g \cdot \nabla T \right]}_C - \underbrace{\frac{R}{c_p p} \nabla^2 \frac{dQ}{dt}}_D \quad (1)$$

The Pacific Decadal Oscillation (PDO; Zhang et al. 1997; Mantua et al. 1997), or more generally the IPO (Power et al. 1999; Deser et al. 2004), is a strong signal of climate variability on the interdecadal time scale. The PDO plays a significant role in the trend variability of the East Asian summer monsoon and the dry-wet conditions of north China, via a phase transition of the PDO (Ma 2007; Li et al. 2010;

Qian and Zhou 2014). Then is the regional variation in surface wind speed trend, which is closely associated with SH tendency, also influenced by the decadal variability in large-scale circulation, PDO? An attempt to identify whether this is the case has been made in the following.

The spring mean PDO index from 1980 to 2015 (Fig. 8a), which is defined by the time series of the leading mode in empirical orthogonal function (EOF) analysis of monthly SST anomalies in the North Pacific Ocean (Zhang et al. 1997; Mantua et al. 1997), is utilized to investigate the effect of PDO on SH. The PDO manifests as a low-frequency El Niño-like pattern of climate variability, with warming in the tropical central and eastern Pacific and cooling over the mid-latitude central and western Pacific during its positive phase (Fig. 8b), and vice versa. And it switched from a warm phase to a cold phase during recent decades (Chen et al. 2008; Burgman et al. 2008; Feng et al. 2010; Meehl and Arblaster 2012; Dai 2013). There was anomalous upward vertical movement (Fig. 8c) associated with surface convergence over the southwest of the TP (Fig. 8d) when the PDO switched from a warm phase to a cold phase. The regression pattern of the wind at 10 m with respect to the PDO multiplied by -1 (Fig. 8d) seems to resemble very closely what the linear trend of surface wind displays (Fig. 6d). The correlation coefficient between the regression field (Fig. 8d) and the linear trend pattern (Fig. 6d) is 0.632 for U wind component and 0.724 for V wind component, both exceeding the 99% confidence level. Meanwhile, the correlation coefficient between the SH trend and SH regression regressed on the normalized PDO, multiplied by -1 , is also significant at the 99% confidence level, with the correlation coefficient

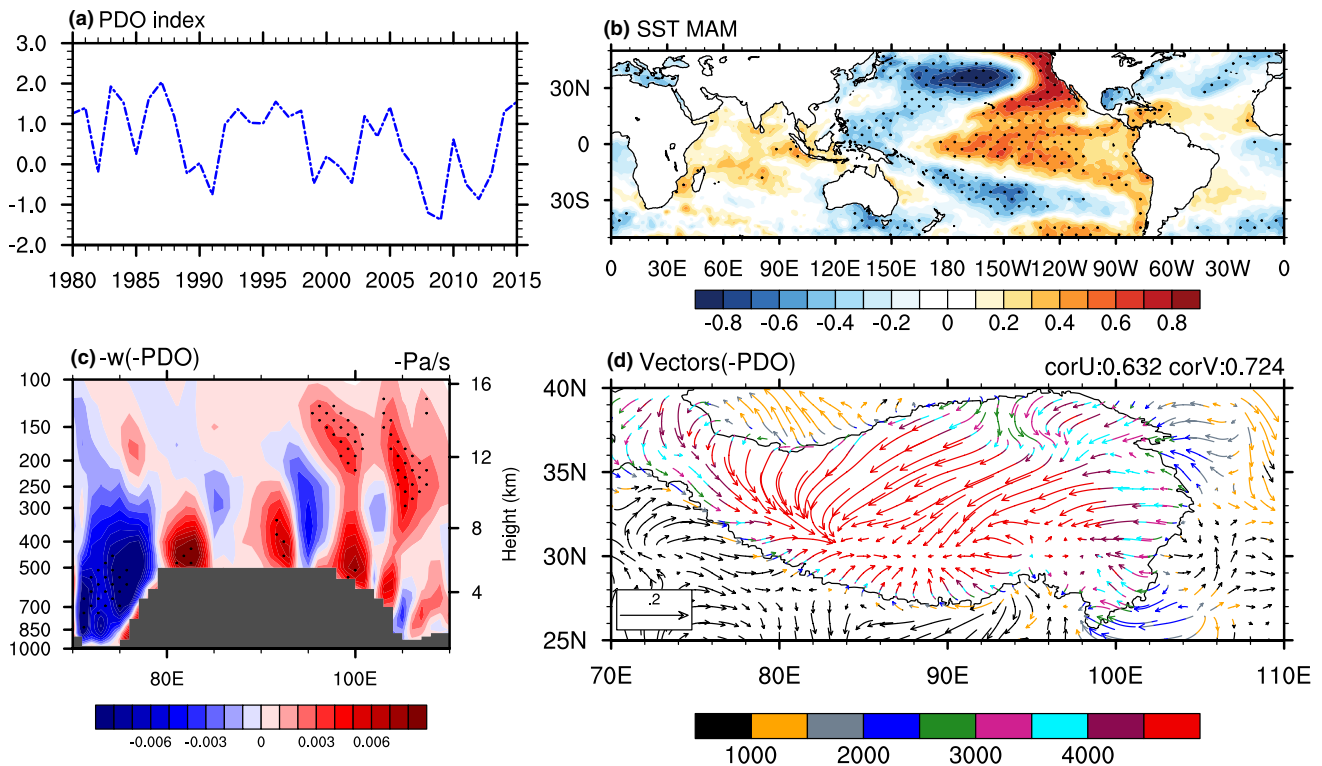


Fig. 8 **a** The time series of spring-mean(MAM) PDO index. **b** The correlation coefficients between the PDO and SST in MAM during 1980–2015. Regression patterns of **c** negative vertical velocity averaged over (31°–32°N) and **d** the wind (vectors) at 10 m regressed

on the normalized PDO index in MAM during 1980–2015. And the PDO index has been multiplied by -1 to facilitate comparison. Dots in **b** and **c** indicate the areas where the values exceed the 95% significance level

of 0.789. This indicates that the PDO may play a significant role in the interdecadal variation of SH over the TP via influence on the surface wind.

To investigate the mechanism for the influence of PDO, the wave activity flux \bar{W} (Formula 2) is calculated by the method developed by Takaya and Nakamura (2001). Readers can refer to literature (Takaya and Nakamura 2001) for details:

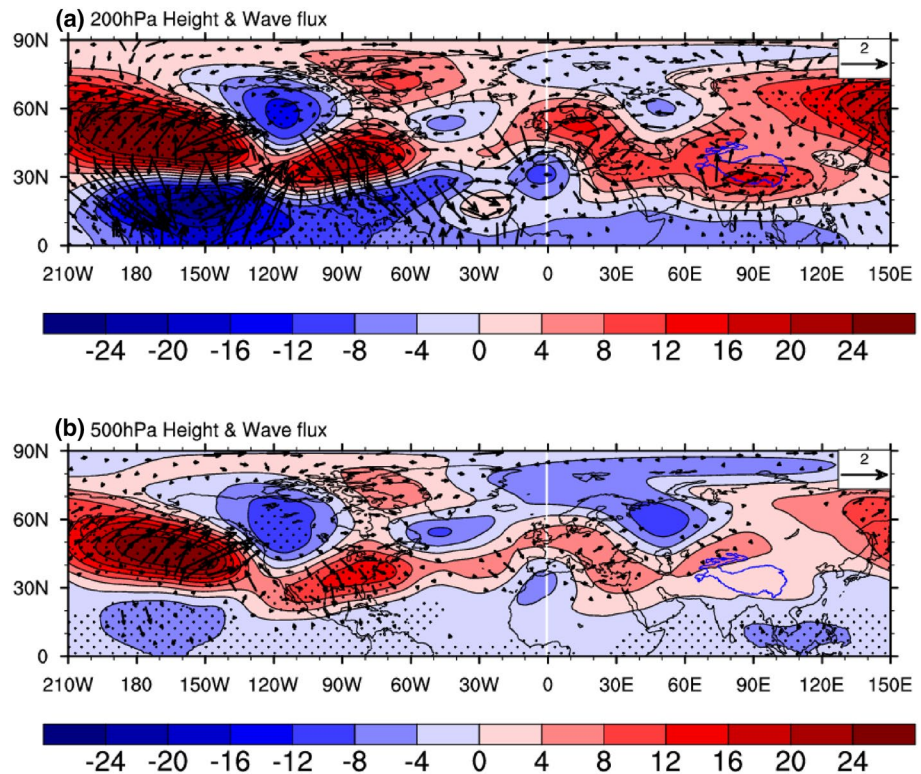
$$\bar{W} = \frac{p \cos \phi}{2 |\bar{U}|} \left(\begin{aligned} & \left[\frac{U}{a^2 \cos^2 \phi} \left[\left(\frac{\partial \psi}{\partial \lambda} \right)^2 - \psi \frac{\partial^2 \psi}{\partial \lambda^2} \right] + \frac{V}{a^2 \cos \phi} \left[\frac{\partial \psi}{\partial \lambda} \frac{\partial \psi}{\partial \phi} - \psi \frac{\partial^2 \psi}{\partial \lambda \partial \phi} \right] \right] \\ & \left[\frac{U}{a^2 \cos \phi} \left[\frac{\partial \psi}{\partial \lambda} \frac{\partial \psi}{\partial \phi} - \psi \frac{\partial^2 \psi}{\partial \lambda \partial \phi} \right] + \frac{V}{a^2} \left[\left(\frac{\partial \psi}{\partial \phi} \right)^2 - \psi \frac{\partial^2 \psi}{\partial \phi^2} \right] \right] \\ & \left. \left[\frac{f_0^2}{N^2} \left\{ \frac{U}{a \cos \phi} \left[\frac{\partial \psi}{\partial \lambda} \frac{\partial \psi}{\partial z} - \psi \frac{\partial^2 \psi}{\partial \lambda \partial z} \right] + \frac{V}{a} \left[\frac{\partial \psi}{\partial \phi} \frac{\partial \psi}{\partial z} - \psi \frac{\partial^2 \psi}{\partial \phi \partial z} \right] \right\} \right] \right) \end{aligned} \right) \quad (2)$$

Figure 9 presents regression field of geopotential height and stationary wave flux against the normalized PDO index (multiplied by -1). During the negative PDO phases, with warming in northwestern Pacific, an alternating pattern of high and low geopotential height arcs propagates eastward from the northwestern Pacific. A positive anomaly centered over 50°N, 170°W is followed by a negative anomaly centered at Canada, alternated by a positive anomaly centered over the southern US. And then the wave train extends from

the North Atlantic to Europe, followed by the propagation northward and eastward from the Arabian Sea to the southwest TP (Fig. 9a). Moreover, this wave pattern has the same phase in the middle and upper troposphere, and it indicates that the vertical structure of those waves is equivalent barotropic (Fig. 9b). Diagnosis of the wave activity flux shows that the wave energy originates above the warm center of the northwestern Pacific and propagates eastward until reaching the southwest TP. And the influence of PDO on the atmospheric circulation over the TP is mainly located in the upper air, where there is a significant increase in geopotential height. In order to maintain mass continuous, the enhancement of divergence in the upper troposphere will result in compensated surface convergence and rising motion over southwest TP (Fig. 8c, d). And that leads to easterly anomaly to the east of the convergence, which consequently results in a decline in the surface wind speed associated with SH over the central and eastern TP, especially in the higher altitude areas.

The warming can cause divergence anomalies there in the upper troposphere. Therefore, the Rossby waves along the wave guide during the negative PDO phases may be resulted from the PDO-related divergence anomalies in the upper troposphere of the northwestern Pacific. To confirm this

Fig. 9 **a** Regression field of MAM geopotential height and stationary wave flux at 200 hPa against the normalized PDO index (multiplied by -1) in MAM during 1980–2015. **b** The same as **a** except for 500 hPa. Values exceeding the 95% significance level are presented in dots. The blue solid curve denotes the TP



mechanism, further studies using model to stimulate this steady downstream Rossby wave train are under way.

5 Summary and discussion

Our analyses reveal the elevation dependent variation in SH trend over the TP and its possible causes. The decreasing trend in SH over the TP above 2000 m altitude is amplified with elevation, especially in spring and summer, which is partially consistent with the conclusion mentioned in previous literature (Duan et al. 2011). Surface wind speed is a stable contributor to the variation in SH trend from lower to higher altitude areas. Meanwhile, the impact of the $T_s - T_a$ on elevation-dependence of SH trend is reinforced at higher-altitude regions. The variation in SH trend contributed by the change of $T_s - T_a$ may be influenced primarily by the diminished sunshine duration and the lessened snow depth in the regions above 2500 m, with the latter being probably more important. As to the portion of variation in SH trend in relation to the change of the surface wind speed, it perhaps is mainly attributed to the dynamic process related to the PDO. The pattern regressed on the negative PDO index exhibits an anomalous wave train, which may develop locally in response to the PDO-associated warm anomalies of the sea surface temperature in northwestern Pacific. The wave energy originates above the warm center of the northwestern Pacific and propagates eastward following the route of

northwestern Pacific–Canada–southern United States–North Atlantic–Europe–Arabian sea–southwest TP. The direct effect of the wave on the regional variability in circulation of the TP is mainly in the upper troposphere. That leads to an enhancement in divergence of the upper troposphere and subsequently a boost in surface convergence and ascending motion over southwest TP. And even more important, there is easterly anomaly to the east of the convergence, which consequently results in a decline in the surface wind speed associated with SH over the TP, especially in the higher altitude areas.

Several issues remain unsolved. First, to confirm the mechanism for the generation of teleconnection wave train, further studies should be conducted in the future via numerical simulations. Second, most meteorological stations over the TP discussed in this article are concentrated over the central and eastern TP due to extremely sparse high-elevation (above 5000 m) observations. Analysis should be conducted for data from satellite data, atmospheric reanalysis or model studies, but these sources have limitations in duration, spatial resolution and so on. So that makes it extremely difficult to determine the elevation dependency for climate variables at high altitude (Rangwala and Miller 2012; Pepin et al. 2015). Besides, we treat the drag coefficient for heat as a constant value in this study, but in fact it is altered relying on several factors, such as atmospheric stability (Guo et al. 2011; Yang et al. 2011b). Thus, there may exist some

uncertainties in results for changes of surface heat flux at high altitude localities.

Acknowledgements The authors thank the CMA for kindly providing the observational data and thank Dr. Yongjie Huang (IAP/CAS) for providing map database. We also thank the anonymous reviewers and editor for their useful comments. This work was supported by the National Natural Science Foundation of China (41425019, 41721004, 41661144016, 91537214, 41775072 and 41505078) and the Public Science and Technology Research Funds Projects of the Ocean (201505013).

References

- Bastiaanssen WGM, Menenti M, Feddes RA, Holtslag AAM (1998) A remote sensing surface energy balance algorithm for land (SEBAL). 1. Formulation. *J Hydrol* 212–213:198–212. [https://doi.org/10.1016/S0022-1694\(98\)00253-4](https://doi.org/10.1016/S0022-1694(98)00253-4)
- Boos WR, Kuang Z (2010) Dominant control of the South Asian monsoon by orographic insulation versus plateau heating. *Nature* 463:218–222
- Burgman RJ, Clement AC, Mitas CM, Chen J, Esslinger K (2008) Evidence for atmospheric variability over the Pacific on decadal timescales. *Geophys Res Lett* 35:L01704. <https://doi.org/10.1029/2007GL031830>
- Ceppi P, Scherrer SC, Fischer AM, Appenzeller C (2010) Revisiting Swiss temperature trends 1959–2008. *Int J Climatol* 32:203–213. <https://doi.org/10.1002/joc.2260>
- Chakraborty A, Nanjundiah RS, Srinivasan J (2002) Role of Asian and African orography in Indian summer monsoon. *Geophys Res Lett* 29(20):1989. <https://doi.org/10.1029/2002GL015522>
- Chakraborty A, Nanjundiah RS, Srinivasan J (2006) Theoretical aspects of the onset of Indian summer monsoon from perturbed orography simulations in a GCM. *Ann Geophys* 24:2075–2089
- Chen LX, Reiter ER, Feng ZQ (1985) The atmospheric heat source over the Tibetan Plateau: May–August 1979. *Mon Weather Rev* 113:1771–1790. [https://doi.org/10.1175/1520-0493\(1985\)113%3C1771:TAHSOT%3E2.0.CO;2](https://doi.org/10.1175/1520-0493(1985)113%3C1771:TAHSOT%3E2.0.CO;2)
- Chen J, Del Genio AD, Carlson BE, Bosilovich MG (2008) The spatiotemporal structure of twentieth-century climate variations in observations and reanalyses. Part II: Pacific pan-decadal variability. *J Clim* 21:2634–2650. <https://doi.org/10.1175/2007JCLI2012.1>
- Cui YF, Duan AM, Liu YM, Wu GX (2015) Interannual variability of the spring atmospheric heat source over the Tibetan Plateau forced by the North Atlantic SSTA. *Clim Dyn* 45:1617–1634. <https://doi.org/10.1007/s00382-014-2417-9>
- Dai A (2013) The influence of the inter-decadal Pacific oscillation on US precipitation during 1923–2010. *Clim Dyn* 41:633–646. <https://doi.org/10.1007/s00382-012-1446-5>
- Dee DP, Uppala SM, Simmons AJ, Berrisford P, Poli P, Kobayashi S, Andrae U, Balmaseda MA, Balsamo G, Bauer P, Bechtold P, Beljaars ACM, Van De Berg L, Bidlot J, Bormann N, Delsol C, Dragani R, Fuentes M, Geer AJ, Haimberger L, Healy SB, Hersbach H, Hlm EV, Isaksen I, Kllberg P, Köhler M, Matricardi M, McNally AP, Monge-Sanz BM, Morcrette JJ, Park BK, Peubey C, De Rosnay P, Tavolato C, Thpaut JN, Vitart F (2011) The ERA-Interim reanalysis: configuration and performance of the data assimilation system. *Q J R Meteorol Soc* 137:553–597. <https://doi.org/10.1002/qj.828>
- Deser C, Phillips AS, Hurrell, JW (2004) Pacific interdecadal climate variability: linkages between the tropics and the North Pacific during boreal winter since 1900. *J Clim* 17:3109–3124. [https://doi.org/10.1175/1520-0442\(2004\)017%3C3109:PICVLB%3E2.0.CO;2](https://doi.org/10.1175/1520-0442(2004)017%3C3109:PICVLB%3E2.0.CO;2)
- Duan AM, Wu GX (2005) Role of the Tibetan Plateau thermal forcing in the summer climate patterns over subtropical Asia. *Clim Dyn* 24:793–807. <https://doi.org/10.1007/s00382-004-0488-8>
- Duan AM, Wu GX (2008) Weakening trend in the atmospheric heat source over the Tibetan Plateau during recent decades. Part I: Observations. *J Clim* 21:3149–3164. <https://doi.org/10.1175/2007JCLI1912.1>
- Duan AM, Li F, Wang MR, Wu GX (2011) Persistent weakening trend in the spring sensible heat source over the Tibetan Plateau and its impact on the Asian summer monsoon. *J Clim* 24:5671–5682. <https://doi.org/10.1175/JCLI-D-11-00052.1>
- Duan AM, Wu GX, Liu YM, Ma YM, Zhao P (2012) Weather and climate effects of the Tibetan Plateau. *Adv Atmos Sci* 29:978–992. <https://doi.org/10.1007/s00376-012-1220-y>
- Duan AM, Wang MR, Lei YH, Cui YF (2013) Trends in summer rainfall over China associated with the Tibetan Plateau sensible heat source during 1980–2008. *J Clim* 26:261–275. <https://doi.org/10.1175/JCLI-D-11-00669.1>
- Feng M, McPhaden MJ, Lee T (2010) Decadal variability of the Pacific subtropical cells and their influence on the southeast Indian Ocean. *Geophys Res Lett* 37:L09606. <https://doi.org/10.1029/2010GL042796>
- Flanner MG, Shell KM, Barlage M, Perovich DK, Tschudi MA (2011) Radiative forcing and albedo feedback from the Northern hemisphere cryosphere between 1979 and 2008. *Nat Geosci* 4:151–155. <https://doi.org/10.1038/ngeo1062>
- Fletcher CG, Zhao H, Kushner PJ, Fernandes R (2012) Using models and satellite observations to evaluate the strength of snow albedo feedback. *J Geophys Res* 117:D11117. <https://doi.org/10.1029/2012JD017724>
- Founda D, Kalimeris A, Pierros F (2014) Multi annual variability and climatic signal analysis of sunshine duration at a large urban area of Mediterranean (Athens). *Urban Clim* 10:815–830. <https://doi.org/10.1016/j.uclim.2014.09.008>
- Giorgi F, Hurrell J, Marinucci M, Beniston M (1997) Elevation dependency of the surface climate change signal: a model study. *J Clim* 10:288–296. [https://doi.org/10.1175/1520-0442\(1997\)010%3C0288:EDOTSC%3E2.0.CO;2](https://doi.org/10.1175/1520-0442(1997)010%3C0288:EDOTSC%3E2.0.CO;2)
- Guo XF, Yang K, Chen YY (2011) Weakening sensible heat source over the Tibetan Plateau revisited: effects of the land–atmosphere thermal coupling. *Theor Appl Climatol* 104:1–12. <https://doi.org/10.1007/s00704-010-0328-1>
- Guo X, Wang L, Tian L, Li X (2017) Elevation-dependent reductions in wind speed over and around the Tibetan Plateau. *Int J Climatol* 37:1117–1126. <https://doi.org/10.1002/joc.4727>
- Hong S, Lakshmi V, Small EE, Chen F, Tewari M, Manning KW (2009) Effects of vegetation and soil moisture on the simulated land surface processes from the coupled WRF/Noah model. *J Geophys Res* 114:D18118. <https://doi.org/10.1029/2008JD011249>
- Hu S, Boos WR (2017a) The physics of orographic elevated heating in radiative-convective equilibrium. *J Atmos Sci* 74(9):2949–2965. <https://doi.org/10.1175/JAS-D-16-0312.1>
- Hu S, Boos WR (2017b) Competing effects of surface albedo and orographic elevated heating on regional climate. *Geophys Res Lett* 44(13):6966–6973. <https://doi.org/10.1002/2016GL072441>
- Hu J, Duan A (2015) Relative contributions of the Tibetan Plateau thermal forcing and the Indian Ocean Sea surface temperature basin mode to the interannual variability of the East Asian summer monsoon. *Clim Dyn* 45:2697–2711. <https://doi.org/10.1007/s00382-015-2503-7>

- Immerzeel WW, Van Beek LPH, Bierkens MFP (2010) Climate change will affect the Asian water towers. *Science* 328(5984):1382–1385. <https://doi.org/10.1126/science.1183188>
- Kothawale DR, Munot AA, Kumar KK (2010) Surface air temperature variability over India during 1901–2007, and its association with ENSO. *Clim Res* 42:89–104. <https://www.jstor.org/stable/24870324>
- Li CF, Yanai M (1996) The onset and interannual variability of the Asian summer monsoon in relation to land–sea thermal contrast. *J Clim* 9:358–375. [https://doi.org/10.1175/1520-0442\(1996\)009%3C0358:TOAIVO%3E2.0.CO;2](https://doi.org/10.1175/1520-0442(1996)009%3C0358:TOAIVO%3E2.0.CO;2)
- Li WP, Wu GX, Liu YM, Liu X (2001) How the surface processes over the Tibetan Plateau affect the summertime Tibetan Anticyclone-numerical experiments. *Chin J Atmos Sci* 25:809–816. <https://doi.org/10.3878/j.issn.1006-9895.2001.06.08> (in Chinese with English abstract)
- Li H, Dai A, Zhou T, Lu J (2010) Responses of East Asian summer monsoon to historical SST and atmospheric forcing during 1950–2000. *Clim Dyn* 34:501–514. <https://doi.org/10.1007/s00382-008-0482-7>
- Liu X, Cheng Z, Yan L, Yin Z (2009) Elevation dependency of recent and future minimum surface air temperature trends in the Tibetan Plateau and its surroundings. *Glob Planet Change* 68:164–174
- Liu YM, Wu GX, Hong JL, Dong B, Duan AM, Bao Q, Zhou LJ (2012) Revisiting Asian monsoon formation and change associated with Tibetan Plateau forcing: II. Change. *Clim Dyn* 39:1183–1195. <https://doi.org/10.1007/s00382-012-1335-y>
- Liu BQ, Wu GX, Mao JY, He JH (2013) Genesis of the South Asian high and its impact on the Asian Summer Monsoon Onset. *J Clim* 26:2976–2991. <https://doi.org/10.1175/JCLI-D-12-00286.1>
- Ma ZG (2007) The interdecadal trend and shift of dry/wet over the central part of north China and their relationship to the Pacific decadal oscillation (PDO). *Chin Sci Bull* 52:2130–2139. <https://doi.org/10.1007/s11434-007-0284-z>
- Manara V, Beltrano MC, Brunetti M, Maugeri M, Sanchez-Lorenzo A, Simolo C, Sorrenti S (2015) Sunshine duration variability and trends in Italy from homogenized instrumental time series (1936–2013). *J Geophys Res Atmos* 120:3622–3641. <https://doi.org/10.1002/2014JD022560>
- Mantua NJ, Hare SR, Zhang Y, Wallace JM, Francis RC (1997) A Pacific interdecadal climate oscillation with impacts on salmon production. *Bull Am Meteorol Soc* 78:1069–1079. [https://doi.org/10.1175/1520-0477\(1997\)078%3C1069:APICOW%3E2.0.CO;2](https://doi.org/10.1175/1520-0477(1997)078%3C1069:APICOW%3E2.0.CO;2)
- Matuszko D (2014) Long-term variability in solar radiation in Krakow based on measurements of sunshine duration. *Int J Climatol* 34:228–234. <https://doi.org/10.1002/joc.3681>
- Meehl GA, Arblaster JM (2012) Relating the strength of the tropospheric biennial oscillation (TBO) to the phase of the Interdecadal Pacific Oscillation (IPO). *Geophys Res Lett* 39:L20716. <https://doi.org/10.1029/2012GL053386>
- Molnar P, Emanuel KA (1999) Temperature profiles in radiative–convective equilibrium above surfaces at different heights. *J Geophys Res Atmos* 104(D20):24265–24271. <https://doi.org/10.1029/1999JD900485>
- Pedelty J, Devadiga S, Masuoka E, Brown M, Pinzon J, Tucker C, Vermote E, Prince S, Nagol J, Justice C, Roy D, Ju J, Schaaf C, Liu J, Privette J, Pinheiro A (2007) Generating a long-term land data record from the AVHRR and MODIS instruments. In: IEEE international geoscience and remote sensing symposium, IEEE, Barcelona, Spain, pp 1021–1025. <https://doi.org/10.1109/IGARS.2007.4422974>
- Pedersen CA, Winther JG (2005) Intercomparison and validation of snow albedo parameterization schemes in climate models. *Clim Dyn* 25:351–362. <https://doi.org/10.1007/s00382-005-0037-0>
- Pepin NC, Lundquist JD (2008) Temperature trends at high elevations: patterns across the globe. *Geophys Res Lett* 35:L14701. <https://doi.org/10.1029/2008GL034026>
- Pepin N, Bradley RS, Diaz HF, Baraer M, Caceres EB, Forsythe N, Fowler H, Greenwood G, Hashmi MZ, Liu XD, Miller JR, Ning L, Ohmura A, Palazzi E, Rangwala I, Schöner W, Severskiy I, Shahgedanova M, Wang MB, Williamson SN, Yang DQ (2015) Elevation-dependent warming in mountain regions of the world. *Nat Clim Change* 5:424–430. <https://doi.org/10.1038/NCLIMATE2563>
- Philippa R, Dürr B, Ohmura A, Ruckstuhl C (2005) Anthropogenic greenhouse forcing and strong water vapor feedback increase temperature in Europe. *Geophys Res Lett* 32:L19809. <https://doi.org/10.1029/2005GL023624>
- Power S, Casey T, Folland C, Colman A, Mehta V (1999) Inter-decadal modulation of the impact of ENSO on Australia. *Clim Dyn* 15:319–324. <https://doi.org/10.1007/s003820050284>
- Qian C, Zhou TJ (2014) Multidecadal variability of North China Aridity and its relationship to PDO during 1900–2010. *J Clim* 27:1210–1222. <https://doi.org/10.1175/JCLI-D-13-00235.1>
- Rangwala I (2013) Amplified water vapour feedback at high altitudes during winter. *Int J Climatol* 33:897–903. <https://doi.org/10.1002/joc.3477>
- Rangwala I, Miller JR (2012) Climate change in mountains: a review of elevation-dependent warming and its possible causes. *Clim Change* 114:527–547. <https://doi.org/10.1007/s10584-012-0419-3>
- Rangwala I, Miller JR, Xu M (2009) Warming in the Tibetan Plateau: possible influences of the changes in surface water vapor. *Geophys Res Lett* 36:L06703. <https://doi.org/10.1029/2009GL037245>
- Rangwala I, Miller JR, Russell GL, Xu M (2010) Using a global climate model to evaluate the influences of water vapor, snow cover and atmospheric aerosol on warming in the Tibetan Plateau during the twenty-first century. *Clim Dyn* 34:859–872. <https://doi.org/10.1007/s00382-009-0564-1>
- Rayner NA, Parker DE, Horton EB, Folland CK, Alexander LV, Rowell DP, Kent EC, Kaplan A (2003) Global analyses of sea surface temperature, sea ice, and night marine air temperature since the late nineteenth century. *J Geophys Res* 108:4407. <https://doi.org/10.1029/2002JD002670>
- Saji NH, Yamagata T (2003) Possible impacts of Indian Ocean dipole mode events on global climate. *Clim Res* 25(2):151–169
- Sanchez-Lorenzo A, Calb J, Martin-Vide J (2008) Spatial and temporal trends in sunshine duration over Western Europe (1938–2004). *J Clim* 21:6089–6098. <https://doi.org/10.1175/2008JCLI2442.1>
- Stanhill G, Cohen S (2005) Solar radiation changes in the United States during the twentieth century: evidence from sunshine duration measurements. *J Clim* 18:1503–1512. <https://doi.org/10.1175/JCLI3354.1>
- Takaya K, Nakamura H (2001) A formulation of a phase-independent wave-activity flux for stationary and migratory quasigeostrophic eddies on a zonally varying basic flow. *J Atmos Sci* 58:608–627. [https://doi.org/10.1175/1520-0469\(2001\)058%3C0608:AFOAPI%3E2.0.CO;2](https://doi.org/10.1175/1520-0469(2001)058%3C0608:AFOAPI%3E2.0.CO;2)
- Wan RJ, Wu GX (2007) Mechanism of the spring persistent rains over southeastern China. *Sci China Ser D Earth Sci* 50:130–144. <https://doi.org/10.1007/s11430-007-2069-2>
- Wan RJ, Zhao BK, Wu GX (2009) New evidences on the climatic causes of the formation of the spring persistent rains over southeastern China. *Adv Atmos Sci* 26:1081–1087. <https://doi.org/10.1007/s00376-009-7202-z>
- Wang MR, Zhou SW, Duan AM (2012) Trend in the atmospheric heat source over the central and eastern Tibetan Plateau during recent decades: comparison of observations and reanalysis data. *Chin Sci Bull* 57:548–557. <https://doi.org/10.1007/s11434-011-4838-8>
- Wang ZQ, Duan AM, Wu GX (2014) Time-lagged impact of spring sensible heat over the Tibetan Plateau on the summer rainfall

- anomaly in East China: case studies using the WRF model. *Clim Dyn* 42:2885–2898. <https://doi.org/10.1007/s00382-013-1800-2>
- Wu GX, Li WP, Guo H (1997) Sensible heat driven air-pump over the Tibetan-Plateau and its impacts on the Asian Summer Monsoon. In: Ye DZ (ed) Collections on the memory of Zhao Jiuzhang. Science Press, Beijing, pp 116–126 (in Chinese)
- Wu GX, Liu YM, Wang TM, Wan RJ, Liu X, Li WP, Wang ZZ, Zhang Q, Duan AM, Liang XY (2007) The influence of mechanical and thermal forcing by the Tibetan Plateau on Asian climate. *J Hydrometeorol* 8:770–789. <https://doi.org/10.1175/JHM609.1>
- Wu GX, Liu YM, He B, Bao Q, Duan AM, Jin FF (2012a) Thermal controls on the Asian summer monsoon. *Sci Rep* 2:404. <https://doi.org/10.1038/srep00404>
- Wu GX, Liu YM, Dong BW, Liang XY, Duan AM, Bao Q, Yu JJ (2012b) Revisiting Asian monsoon formation and change associated with Tibetan Plateau forcing: I. Formation. *Clim Dyn* 39:1169–1181. <https://doi.org/10.1007/s00382-012-1334-z>
- Wu GX, Guan Y, Liu YM, Yan JH, Mao JY (2012c) Air-sea interaction and formation of the Asian summer monsoon onset vortex over the Bay of Bengal. *Clim Dyn* 38:261–279. <https://doi.org/10.1007/s00382-010-0978-9>
- Wu GX, Duan AM, Liu YM, Mao JY, Ren RC, Bao Q, He B, Liu BQ, Hu WT (2014) Tibetan Plateau climate dynamics: recent research progress and outlook. *Natl Sci Rev* 2:100–116. <https://doi.org/10.1093/nsr/nwu045>
- Wu GX, Zhuo HF, Wang ZQ, Liu YM (2016) Two types of summertime heating over the Asian large-scale orography and excitation of potential-vorticity forcing I. Over Tibetan Plateau. *Sci China Earth Sci* 59:1996–2008. <https://doi.org/10.1007/s11430-016-5328-2>
- Yan L, Liu X (2014) Has climatic warming over the Tibetan Plateau paused or continued in recent years? *J Earth Ocean Atmos Sci* 1:13–28
- Yanai M, Li CF, Song ZS (1992) Seasonal heating of the Tibetan Plateau and its effects on the evolution of the Asian summer monsoon. *J Meteorol Soc Jpn* 70:319–351. https://doi.org/10.2151/jmsj1965.70.1B_319
- Yang K, Guo XF, He J, Qin J, Koike T (2011a) On the climatology and trend of the atmospheric heat source over the Tibetan Plateau: an experiments-supported revisit. *J Clim* 24:1525–1541. <https://doi.org/10.1175/2010JCLI3848.1>
- Yang K, Guo XF, Wu BY (2011b) Recent trends in surface sensible heat flux on the Tibetan Plateau. *Sci China Earth Sci* 54:19–28. <https://doi.org/10.1007/s11430-010-4036-6>
- Yao TD, Thompson L, Yang W, Yu WS, Gao Y, Guo XJ, Yang XX, Duan KQ, Zhao HB, Xu BQ, Pu JC, Lu AX, Xiang Y, Kattel DB, Joswiak D (2012) Different glacier status with atmospheric circulations in Tibetan Plateau and surroundings. *Nat Clim Change* 2:663–667. <https://doi.org/10.1038/nclimate1580>
- Ye DZ, Wu GX (1998) The role of the heat source of the Tibetan Plateau in the general circulation. *Meteorol Atmos Phys* 67:181–198. <https://doi.org/10.1007/BF01277509>
- Yeh TC, Gao YX (1979) Qinghai-Xizang Plateau meteorology. Science Press, Beijing, pp 1–278 (in Chinese)
- Yeh TC, Lo SW, Chu PC (1957) The wind structure and heat balance in the lower troposphere over Tibetan Plateau and its surrounding. *Acta Meteorol Sin* 28:108–121. <https://doi.org/10.11676/qxxb1957.010> (in Chinese with English abstract)
- Zar JH (1999) Biostatistical analysis, 4th edn. Prentice-Hall, Upper Saddle River
- Zhang Y, Wallace J M, Battisti DS (1997) ENSO-like interdecadal variability: 1900–93. *J Clim* 10:1004–1020. [https://doi.org/10.1175/1520-0442\(1997\)010%3C1004:ELIV%3E2.0.CO;2](https://doi.org/10.1175/1520-0442(1997)010%3C1004:ELIV%3E2.0.CO;2)
- Zheng D, Der Velde RV, Su Z, Booij MJ, Hoekstra AY, Wen J (2014) Assessment of roughness length schemes implemented within the Noah land surface model for high-altitude regions. *J Hydrometeorol* 15:921–937. <https://doi.org/10.1175/JHM-D-13-0102.1>
- Zhu LH, Huang G, Fan GZ, Qu X, Zhao GJ, Hua W (2017) Evolution of surface sensible heat over the Tibetan Plateau under the recent global warming hiatus. *Adv Atmos Sci* 34:1249–1262. <https://doi.org/10.1007/s00376-017-6298-9>